Published in final edited form as:
Toxicol Appl Pharmacol. 2009 October 1; 240(1): 88–98. doi:10.1016/j.taap.2009.07.009.

In Vivo Toxicity Studies of Europium Hydroxide Nanorods in Mice

Chitta Ranjan Patra[1,*], **Soha S. Abdel Moneim**[2,3], **Enfeng Wang**[1], **Shamit Dutta**[1], **Sujata Patra**[1], **Michal Eshed**[4], **Priyabrata Mukherjee**[1,5], **Aharon Gedanken**[4], **Vijay H Shah**[2], and **Debabrata Mukhopadhyay**[1,5]

[1] Department of Biochemistry and Molecular Biology, 200 First Street S.W, Guggenheim 1034, Mayo Clinic College of Medicine, Mayo Foundation, Rochester, MN 55905, USA

[2] Gastroenterology and Hepatology, GI Research Unit, 200 First Street S.W, Guggenheim 1034, Mayo Clinic College of Medicine, Mayo Foundation, Rochester, MN 55905, USA

[4] Department of Chemistry and Kanbar Laboratory for Nanomaterials, Bar-Ilan University Center for Advanced Materials and Nanotechnology, Bar-Ilan University, Ramat-Gan 52900, Israel

[5] Department of Biomedical Engineering, 200 First Street S.W, Guggenheim 1334, Mayo Clinic College of Medicine, Mayo Foundation, Rochester, MN 55905, USA

Abstract

Lanthanide nanoparticles and nanorods have been widely used for diagnostic and therapeutic applications in biomedical nanotechnology due to their fluorescence properties and pro-angiogenic to endothelial cells, respectively. Recently, we have demonstrated that europium (III) hydroxide [$Eu^{III}(OH)_3$] nanorods, synthesized by the microwave technique and characterized by several physico-chemical techniques, can be used as pro-angiogenic agents which introduce future therapeutic treatment strategies for severe ischemic heart/limb disease, and peripheral ischemic disease. The toxicity of these inorganic nanorods to endothelial cells was supported by several *in vitro* assays. To determine the *in vivo* toxicity, these nanorods were administered to mice through intraperitoneal injection (IP) everyday over a period of seven days in a dose dependent (1.25 to 125 $mgKg^{-1}day^{-1}$) and time dependent manner (8–60 days). Bio-distribution of europium elements in different organs was analyzed by inductively coupled plasma mass spectrometry (ICPMS). Short-term (S-T) and long-term (L-T) toxicity studies (mice sacrificed on day 8 and 60 for S-T and L-T, respectively) show normal blood hematology and serum clinical chemistry with the exception of a slight elevation of liver enzymes. Histological examination of nanorod treated vital organs (liver, kidney, spleen and lungs) showed no or only mild histological changes that indicate mild toxicity at the higher dose of nanorods.

*Address for correspondence: Chittaranjan Patra[1], Ph.D, Assistant Professor, 200 First Street S.W, Guggenheim 1321A, Mayo Clinic College of Medicine, Mayo Foundation, Rochester, MN 55905, USA, patra.chittaranjan@mayo.edu, Phone: +1-507-284-9116, Fax: +1-507- 293-1058.

[3]Present address: Soha S Abdelmonein, lecturer of Tropical medicine and gasteroentrology, Assuit university, Assuit, Egypt.

CONFLICT OF INTEREST STATEMENT

Mayo Foundation for Medical Education and Research has filed a patent (Patent Application No.# PCT/US2007/075926) entitled “RARE EARTH NANOPARTICLES” which lists Drs. Chittaranjan Patra, Priyabrata Mukherjee and Debabrata Mukhopadhyay as inventors. Dr. Patra, Dr. Mukhopadhyay, and Dr. Mukherjee disclosed that they and Mayo Clinic have a financial interest in the technology related to this research. That technology has been licensed to a privately held biotechnology company. Mayo Clinic holds equity in this company, and Mayo Clinic and Drs. Patra, Mukherjee and Mukhopadhyay have contractual rights to receive future royalties from the licensing of this technology.”

Keywords

Europium(III)hydroxide nanorods; $Eu^{III}(OH)_3$; Microwave; HUVECs; *In vivo* toxicity; Histology; ICPMS

INTRODUCTION

Nanoscience and nanotechnology are cutting edge technologies that are devoted to understand, create, design and use material structures, devices and systems at the atomic, molecular, or macromolecular range (~1–100 nanometers) with fundamentally new properties and function (Alivisatos *et al.*, 1996; Craighead, 2000; Alivisatos, 2004; Patra *et al.*, 2005; Patra *et al.*, 2006; Patra *et al.*, 2007; Patra *et al.*, 2008a; Patra *et al.*, 2008b; Patra *et al.*, 2008c; Patra *et al.*, 2008d; Patra *et al.*, 2008e). Nanomedicine is the biomedical application of nanotechnology. Nanoparticles or nanorods have been widely used for useful research tools, advanced drug delivery systems (DDS), and new ways to detect and treat disease or repair damaged tissues and cells (Alivisatos *et al.*, 1996; Bruchez *et al.*, 1998; Parak *et al.*, 2003; Alivisatos, 2004; Gao *et al.*, 2004; Thrall, 2004; Gao *et al.*, 2005; Jain, 2005a; Jain, 2005b; Medintz *et al.*, 2005; Michalet *et al.*, 2005; Prescher and Bertozzi, 2005; Patra *et al.*, 2008a; Patra *et al.*, 2008b; Patra *et al.*, 2008c). In this context, several groups including our group have demonstrated that lanthanide (Eu, Tb, Gd) elements/nanoparticles play important roles in biology and medicine due to their unique physical, chemical, and electronic properties (Misra *et al.*, 2004; Sigel and Sigel, 2004; Authors, 2006; Patra *et al.*, 2006; Thompson and Orvig, 2006; Yu *et al.*, 2006; Patra *et al.*, 2007; Patra *et al.*, 2008b; Patra *et al.*, 2009). Recently, we have demonstrated that europium hydroxide [$Eu^{III}(OH)_3$] nanorods (inorganic nanorods) exhibit significant pro-angiogenic activities (Patra *et al.*, 2008b). It is well established that the most important objective of angiogenesis (process involving the growth of new blood vessels from pre-existing vasculature) is to induce or stimulate vessel growth in patients with conditions characterized by insufficient blood flow, such as ischemic heart disease (IHD) and peripheral vascular diseases(Folkman and Shing, 1992; Folkman, 1993; Folkman, 1995; Risau, 1997; Isner and Losordo, 1999; Yancopoulos *et al.*, 2000; Chavakis and Dimmeler, 2002; Dardik *et al.*, 2005 Basu, 2001 #42; Folkman, 1974). Considering the overall impact of angiogenesis in our health care system, the pro-angiogenic properties of $Eu^{III}(OH)_3$ nanorods could be used to develop new treatment strategies for ischemic heart/limb disease, (Huston *et al.*, 1999; Jones *et al.*, 2002; Ebrahimian *et al.*, 2006) in the near future. However, applications of any nanoparticles and nanorods in biomedical technology require that the nanoparticles/nanorods should be non-toxic *in vivo*. It is reported that exposure to certain nanomaterials and metallic salts of lanthanides might lead to adverse biological effects; this appears to be dependent upon the chemical and physical properties of the material (Ogawa *et al.*, 1995; Shimada *et al.*, 1996; Hirano and Suzuki, 1996 ; Jaiswal *et al.*, 2003; Derfus *et al.*, 2004; Gao *et al.*, 2004; Gao *et al.*, 2005). Our preliminary results demonstrated that these nanorods are not toxic to endothelial cells as observed by apoptosis assay and other *in vitro* assays (Patra *et al.*, 2006; Patra *et al.*, 2007; Patra *et al.*, 2008b) as well as *in vivo* assay (CAM assay) (Patra *et al.*, 2008b). These encouraging findings prompted us to further evaluate the *in vivo* toxicity in mice models. There are some reports on the toxicity study of lanthanide compounds (salts or chelates) (Haley *et al.*, 1965; Ogawa *et al.*, 1995; Shimada *et al.*, 1996; Hirano and Suzuki, 1996 ; Zhang *et al.*, 2002). Although Haley et al. in 1965 (Haley *et al.*, 1965) reported the pharmacological and toxicological properties of europium chloride in mice models, there is not a single report on *in vivo* toxicity study using lanthanide nanoparticles or nanorods, especially $Eu^{III}(OH)_3$ nanorods. Again, the efficacy of these $Eu^{III(}OH)_3$ nanorods in promoting angiogenesis in the mammalian heart/limb and its feasibility, safety, and bio-availabilities with *in vivo* use has not been established. Since nanoparticles may interact with biological systems

in unforeseen ways, an *in vivo* toxicity study of $Eu^{III}(OH)_3$ is one of the important steps before applying these nanomaterials for *in vivo* use.

In this present article our goal is to study *in vivo* bio-toxicity and bio-availabilities of $Eu^{III}(OH)_3$ nanorods in mice models in a systematic way. We have examined short-term (S-T: mice sacrificed on day eight after seven days of consecutive IP injections of nanorods) (acute) and long-term (L-T: mice sacrificed on day 60) (chronic) *in vivo* toxicity of $Eu^{III}(OH)_3$ nanorods and their bio-availabilities in mice models. We have collected the various vital organs (liver, spleen, lungs, kidney) and performed histopathological examination using H&E staining to compare the acute and chronic toxicity of controlled tissue vs. nanorod treated tissue. We have also determined bio-distribution of the europium element in different organs using inductively coupled plasma mass spectrometry (ICP-MS). Intraperitoneal (IP) injection of $Eu^{III}(OH)_3$ nanorods in mice at different doses (1.25 to 125 $mgKg^{-1}day^{-1}$) has not shown any biochemical and hematological toxicities with the exception of a slight elevation of liver enzymes. Histological examination of nanorod-treated vital organs (liver, kidney, spleen and lungs) assayed on day eight (S-T) or 60 (L-T) showed none or only mild histological changes that indicated mild toxicity with the higher dose of nanorods. The remarkable findings of pro-angiogenic and fluorescence properties and non-toxic behavior of $Eu^{III}(OH)_3$ nanorods suggests that these nanorods could be used for future therapeutic alternative treatment strategies for severe ischemic heart disease, peripheral ischemic disease, and limb ischemic disease.

METHODS

Materials

Europium (III)nitrate hydrate [$Eu(NO_3)_3.xH_2O$, 99.99%] and aqueous ammonium hydroxide [aq.NH_4OH, 28–30%] were purchased from Aldrich, USA and were used without further purifications. The human umbilical vein endothelial cells (HUVEC) and its individual components for making EBM complete media were purchased from Cambrex Bio Science Walkersville, Inc, MD, USA. TUNEL labeling assay kit (In Situ Cell Death Detection Kit: Cat. No.#12 156 792 910) was purchased from Roche Applied Science, IN, USA.

Synthesis of $Eu^{III}(OH)_3$ Nanorods by Microwave Irradiation

Synthesis of $Eu^{III}(OH)_3$ nanorods was carried out in a modified domestic microwave oven (DMO) prepared using an interaction in an aqueous solution of Europium(III)nitrate and aq.NH_4OH using microwave (MW) irradiation (Patra *et al.*, 2008b). In a typical synthesis, 10 ml of aqueous NH_4OH were added to 20 ml of a 0.05 (M) aqueous solution of Eu(III)nitrate (pH = 5.5) in a 100 ml round-bottomed flask and were irradiated for 5 to 60 min with 60% of the instrument's power (on/off irradiation cycles ratio of 3/2) in order to control the reaction and reduce the risk of superheating the solvent. A white and colloidal precipitate, without any special morphology, was obtained upon the addition of NH_4OH to the Eu(III) nitrate solution in absence of MW heating. The pH of the solution before and after the reaction was measured and these were 9.4 and 7.5, respectively. The microwave refluxing apparatus is a modified domestic microwave oven (GOLD STAR 1000W with a 2.45 GHz) (Matsumurainoue *et al.*, 1994; Patra *et al.*, 2008b) In the post-reaction treatment the resulting products were collected, centrifuged, washed several times using distilled water, and then dried overnight under vacuum at room temperature. The yield of the as-prepared products was more than 95%.

Nanorod Solution Preparation

100 mg of solid crystalline $Eu^{III}(OH)_3$ nanorods were added into 10 ml of sterile TE (tris-EDTA) buffer and kept five min in a sonicator bath to make a homogeneous suspension of 10 mg/ml (stock solution). The freshly prepared suspension in TE buffer was used for all cell culture experiments and *in vivo* toxicity experiments.

Detection of Endotoxin

The milipore H_2O, used for all experiments in our research, was tested for endotoxin using the Gel clot method according to manufacturer's instructions (Cat # GS 250Cape Cod Associates, Cape Cod). The formation of a gel-clot indicates the presence of endotoxin in a sample. However, we have not found any gel-clot confirming the absence of endotoxin in the water. Similarly, prior to incubation with endothelial cells (HUVECs) for apoptosis studies, we tested the nanorods suspension in TE-buffer for possible endotoxin contamination.

Cell Culture Experiments and TUNEL Assay

In the TUNEL assay, cells were seeded into 6-well plates at a density of 10^5 in 2 ml of medium per well and grown overnight on cover slips at 37°C and 5% CO2 in EBM complete media. The cells were then treated with $Eu^{III}(OH)_3$ nanorods and allowed for another 24 hours of incubation at different concentrations (0–100 μg/ml). After 24 hrs of incubation, the cover slips were rinsed extensively with PBS, and cells were fixed with freshly prepared 4% para-formaldehyde in PBS for 15 min at room temperature and then re-hydrated with PBS. Once all the cells were fixed, the cover slips were mounted onto glass slides with Fluor Save mounting media and used for confocal microscopy. For the TUNEL assay, cells were mounted onto glass slides with mounting media containing DAPI (4′-6-Diamidino-2-phenylindole) and examined with confocal microscopy according to the manufacturer's instructions. The apoptotic cells were counted (6 fields per sample) and photographed using a digital fluorescence camera.

Animals

Six to eight-week-old male wild type mice (C57BL6) were purchased from the National Cancer Institute (NCI), USA. All mice experiments were done under protocols approved by the Mayo Clinic Institutional Animal Care and Use Committee (IACUC).

Treatment of $Eu^{III}(OH)_3$ Nanorods in Mice

$Eu^{III}(OH)_3$ nanorods suspension in TE buffer with different concentrations (1.25 $mgKg^{-1}day^{-1}$, 12.5 $mgKg^{-1}day^{-1}$ and 125 $mgKg^{-1}day^{-1}$) was administered to each mouse through intraperitonial injection (IP) every day with the help of a tuberculin syringe over a period of seven days. In the control group, an equal volume of TE buffer was injected through IP in the same way. Each group contained ten mice. Mice were classified as a short-term (S-T) toxicity study (acute toxicity study) and a long-term (L-T) toxicity study (chronic toxicity study) where mice were sacrificed on day 8 and day 60, respectively, for examination for biochemical toxicity studies, hematological toxicity studies, and histological studies. Mice were allowed free access to autoclaved standard pellet food and sterile water throughout the experiments. Animals were weighed and observed regularly for clinical signs and monitored daily for morbidity and mortality. At least ten mice were used in each set.

We would like to introduce why we have chosen this wide dose range (1.25–125 $mgKg^{-1}day^{-1}$) of $Eu^{III}(OH)_3$ nanorods. According to existing literature, we have not found a single report on *in vivo* toxicity of lanthanide nanoparticles or nanorods, especially $Eu^{III}(OH)_3$ nanorods. Cell proliferation experiments showed that up to 100 μg of nanorods are not toxic to endothelial cells according to our published literature. (Patra *et al.*, 2008b) However, in the case of the *in vivo* angiogenesis (CAM assay: chick chorioallantoic membrane) assay, we have observed the toxic effect of nanorods at a concentration of 20 μg. These observations indicate that the toxic effect of $Eu^{III}(OH)_3$ nanorods can vary from the *in vitro* to the *in vivo* condition. Therefore, in order to determine the systematic *in vivo* toxicity of these inorganic nanorods in mice models, we have selected three doses (wide range) from 1.25 $mg^{-1}Kg^{-1}day^{-1}$ (lowest) to 125 $mg^{-1}Kg^{-1}day^{-1}$(highest). Ogawa et al. (Ogawa *et al.*, 1995) experimented with a toxicity study of europium chloride salt (not nanorods/particles) in rats at

a maximum dose of 1000 mg/Kg/day, and they concluded that the no-observed effect level was 200 mg/Kg/day. Again, Bruce et al. (Bruce *et al*., 1963) reported an intraperitoneal LD50 for europium nitrate in female mice of 320 mg/kg and in female rats of 210 mg/kg. The oral LD50 in the latter species was 75 Gm. This is also another reason for using a wider dose range (1.25–125 $mg^{-1}Kg^{-1}day^{-1}$) of $Eu^{III}(OH)_3$ nanorods in order to study their biocompatibility, efficacy, feasibility, safety, and bio-availability.

We have chosen the administration of $Eu^{III}(OH)_3$ nanorods by intraperitoneal (IP) injection as it is predominantly used for its ease of administration compared to other parenteral methods during animal testing for the administration of systemic drugs and fluids. Additionally, we can administer a large volume of $Eu^{III}(OH)_3$ nanorod suspensions (~100 μl) to the mice if we choose this IP route compared to the intravenous (IV) method. For our *in vivo* toxicity experiments, we have injected a constant volume of 100 μl of nanorod solution to the control as well as the experimental group. However, we can't inject this large volume of solution via the intravenous (IV) route. For these reasons, we have chosen IP administration vs. the intravenous route.

Hematological Analysis and Serum Biochemical Analysis

Mice were sacrificed on day eight (short-term) and on day 60 (long-term) from the date of injection to determine the acute toxicity and chronic toxicity of $Eu^{III}(OH)_3$ nanorods through examination of their blood chemistry profiles. Blood was collected by intracardiac puncture following anesthesia with ketamine-xylazine. Whole blood was immediately heparinized for hematological toxicity. Hematology analysis includes CBC without differential hemoglobin (g/dL), hematocrit (%), erythrocytes [x10(12)/L, mean cell volume (MCV) (fL), RBC distribution width (%), Leukocytes [x10(9)/L] and platelet count [x10(9)/L]. In another set of experiments whole blood was placed in a clotted vial and centrifuged, and collected serum was submitted for biochemical analysis. Serum biochemical analysis was carried out to determine the serum level of alkaline phosphates (ALP), aspartate aminotransferase (AST), alanine aminotransferase (ALT), Phosphorus (Inorganic), calcium, albumin, creatinine (CRN), glucose, total protein (TP), total bilirubin (TBLi), blood urea nitrogen (BUN), etc (Hainfeld *et al*., 2006).

Histopathology

After intraperitonial injection (IP) each day with different doses (0 $mgKg^{-1}day^{-1}$, 1.25 $mgKg^{-1}day^{-1}$, 12.5 $mgKg^{-1}day^{-1}$ and 125 $mgKg^{-1}day^{-1}$) over a period of seven days, the animals were sacrificed. The vital organs (liver, kidney, spleen and lungs) were collected from the mice sacrificed on day eight (S-T toxicity study) and day 60 (L-T toxicity study) and fixed with a 10% formalin neutral buffer solution, embedded in paraffin, and cut into 5-μm-thick sections. Sections were stained with hematoxylin and eosin (H&E) staining for general histology according to our published literature (Reinders *et al*., 2003). Reporting and representation of histologic findings is dependent upon the subjective judgment of the investigator. To avoid this to some extent, the evaluation should be blinded and the slides should be randomized. Therefore, the slides for H&E staining were randomized using some secret code numbers and evaluated blindly by a pathologist. The results were again re-analyzed by another pathologist in the same way.

Bio-distribution of Europium Nanorods—We have also collected the vital organs (liver, kidney, spleen and lung) separately and submitted them for inductively coupled plasma mass spectrometry (ICP-MS) analysis for the determination of europium elements in order to evaluate the bio-distribution of europium in different vital organs.

CHARACTERIZATION TECHNIQUES

Characterization techniques for $Eu^{III}(OH)_3$ nanorods are described briefly as follows.

X-ray diffraction (XRD)

The structure and phase purity of the as–synthesized samples were determined by X-ray diffraction (XRD) analysis using a Bruker AXS D8 Advance Powder X-ray diffractometer (using $CuK_{\alpha}\lambda$ =1.5418 Å radiation).

Transmission electron microscopy (TEM) study

The particle morphology (microstructures of the samples) was studied with TEM on a FEI Technai 12 operating at 80KV.

Inductively coupled plasma mass spectrometry (ICPMS)

The collected organs (liver, kidney, spleen, lungs) were weighed and then dissolved in a 75% HNO3 solution (by volume) such that the amount of acid added was equal to ten times the weight of the sample (wet). The samples were then heated overnight at 50 °C with occasional venting by loosening the caps. The resulting solution was then diluted with deionized water up to a total dilution of 200 times the original weight of the sample. These solutions were again heated overnight at 50 °C. Finally, the solutions were cooled and diluted another 10 fold with the addition of yttrium as an internal standard element and subsequently analyzed on the ICP-MS. We used calibration standards at 0.1, 1.0, and 10.0 ppm Eu for the analysis. We analyzed the samples at three different Eu emission lines (Eu_{3819}, Eu_{3907} and Eu_{41290}) to insure that there were no spectral interferences. All lines were observed from an axial viewpoint of the plasma to increase sensitivity. The mean and standard deviation data were based on five replicates per sample. Several of the samples were re-diluted and analyzed as duplicates to insure reproducibility.

Statistics

Mean and standard deviations were calculated. We have calculated the P values using the ‘Student-Newman-Keuls Multiple Comparisons Test’ (ANOVA) by comparing different groups (control group vs. treatment groups), and we found that these values are considered not significant ($P > 0.05$) (Table 1–4).

RESULTS AND DISCUSSION

The crystal structure of the as-synthesized products were identified using X-ray diffraction (XRD) analysis (Fig. 1). XRD pattern of as-synthesized nanorods, obtained after 60 min MW heating indicated the crystalline nature of the product (Fig. 1). All reflections are distinctly indexed to a pure hexagonal phase of $Eu^{III}(OH)_3$ materials. No peaks from other phases were detected. The diffraction peaks were consistent with the standard data files (the JCPDS card No. 01-083-2305) for all reflections.

The morphologies of the as-synthesized materials were characterized by low-resolution transmission electron microscopy (LRTEM). Fig. 2(a–b) depicts the TEM images of $Eu^{III}(OH)_3$ materials at low magnification (Fig. 2a) and high magnification (Fig. 2b), respectively. The TEM images clearly show that the $Eu^{III}(OH)_3$ materials entirely consists of nanorods with a diameter 35– 50 nm and length in 200–300 nm.

The exact mechanism for the formation of $Eu(OH)_3$ nanorods using microwave irradiation under a solvothermal condition needs further investigation. $Eu(OH)_3$ nanorods that were fabricated have a hexagonal crystal structure similar to that of ZnO (Huang *et al.*, 2001) and

$Ln(OH)_3$ (Wang and Li, 2002; Xu *et al.*, 2003) and $LnPO_4$ (Ln = La -Dy) nanowires (Fang *et al.*, 2003), which are well-known to exhibit anisotropic growth. In this solution phase process, the morphology of the final product was largely determined by the anisotropic nature of the building block, that is, the 1-D characteristic of the infinite hexagonal chains in the crystalline phase. $Eu(OH)_3$ has a hexagonal crystal structure; therefore, the formation of the $Eu(OH)_3$ nanorods can be explained by its highly anisotropic growth.

We suggest that the high microwave susceptibility of water (dielectric constant e = 80.4) makes it an excellent microwave-absorbing agent, thus leading to high heating rates and significantly shortened reaction times. The movement and polarization of water molecules under the rapidly changing electric field of the microwave reactor may result in transient, anisotropic microdomains for the reaction system, facilitating the anisotropic growth of $Eu(OH)_3$ nanorods (Patra *et al.*, 2005; Mazloumi *et al.*, 2009).

In order to determine the chemical nature of the as-synthesized products, it was further characterized by thermo gravimetric analysis (TGA) and differential scanning calorimetric (DSC) analysis according to our earlier literature (Patra *et al.*, 2008b). The combined results of XRD, TEM, TGA and DSC indicating that as-synthesized product is crystalline $Eu^{III}(OH)_3$ nanorods.

Recently, we have already demonstrated the pro-angiogenic properties of $Eu^{III}(OH)_3$ nanorods through various *in vitro* (such as cell proliferation assay using [^{3}H]-Thymidine, cell cycle assay) and *in vivo* analyses (CAM: chick chorioallantoic membrane assays) (Patra *et al.*, 2008b). Like other pro-angiogenic cytokines, these nanorods promote *in vitro* endothelial cell proliferation and *in vivo* angiogenic sprouting in CAM assays. The internalization of $Eu^{III}(OH)_3$ nanorods inside the cells was visualized with a TEM according to previously published procedures (McDowell and Trump, 1976; Spurr, 1969). We have already demonstrated that mitogen activated protein kinase (MAPK) activation and formation of reactive oxygen species (ROS) is the plausible mechanism for inorganic nanorods induced angiogenesis.

One of the main purposes of the current study was to evaluate the potential toxicity of Eu $(OH)_3$ nanorods. In order to obtain detailed information of toxicity, we performed *in vivo* serum biochemical analysis, blood chemistry, histopathological examination, and *in vitro* apoptosis assays. The toxicity of these inorganic nanorods to endothelial cells was further supported by apoptosis assay/TUNEL assay (dUTP nick-end labeling) and is shown in Fig. 3. To determine the toxicity of these nanorods, we performed the TUNEL assay on HUVECs in the presence of these nanorods according to published literatures (Wu *et al.*, 2002;Chen *et al.*, 2006;Patra *et al.*, 2006;Patra *et al.*, 2007;Patra *et al.*, 2008b). As we have already demonstrated cell viability tests using a trypan blue dye exclusion test, apoptosis assay, cell proliferation assay, cell cycle assay, etc. in our published literature (Patra *et al.*, 2008b), therefore we have not presented the similar *in vitro* data in this article. Fig. 3.a illustrates the TUNEL assay of HUVECs treated with tris-EDTA buffer (−Ve control experiment) where we have not found any red apoptotic nuclei indicating no apoptosis. Fig. 3.b shows the TUNEL assay of HUVECs treated with camptothecin for 4h at 37°C as a positive inducer where red nuclei indicate the apoptosis of all HUVEC cells. Apoptosis assay of HUVECs treated with $Eu^{III}(OH)_3$ nanorods (50 μg/mL) were presented in Fig. 3c where we did not observe any apoptotic cells. However, HUVECs treated with nanorods at the concentration of 100 μg/mL (Fig. 3.d) show some red apoptotic cells indicating that a higher concentration of nanorods are apoptotic (~8%) to endothelial cells. Results from the TUNEL assay clearly demonstrated that at concentrations up to 50 μg/ml of $Eu^{III}(OH)_3$ nanorods, there was no induction of apoptosis in HUVECs.

In vivo toxicity

Recently, the potentially hazardous health effects of nanoparticles are emerging issues among toxicologists and regulatory authorities. Nanotechnology will indeed develop in areas where potential advantages would exceed potential risks and where the potential risks are limited and can be addressed (Roco, 2003). Current approaches strongly suggest that consequences of nanotechnology are best addressed within the existing system applications such as biology, chemistry, or electronics. The aim of current study is to determine the distribution pattern and potential toxicity of inorganic nanorods using $Eu^{III}(OH)_3$ nanorods and histopathological changes of organs in the presence of these nanorods. $Eu^{III}(OH)_3$ nanorod suspension in TE buffer with different concentrations (1.25 $mgKg^{-1}day^{-1}$, 12.5 $mgKg^{-1}day^{-1}$ and 125 $mgKg^{-1}day^{-1}$) was administered to each mouse through intraperitonial injection (IP) each day over a period of seven days. Briefly, on day eight and day 60 toxicity studies using 60 mice with intraperitonial injection of $Eu^{III}(OH)_3$ nanorods (maximum dose125 $mgKg^{-1}day^{-1}$) showed normal hematology (Table-1 & -3) and blood chemistry (Table -2 & -4). Histological examination of vital organs including liver, kidney, spleen, and lungs from each mouse, assayed on day eight or day 60 after injection of nanorods showed none or only mild histological changes indicating evidence of mild toxicity at the highest dose of nanorods (Fig. 4.a–p). None of those mice were dead; and we have not observed any significant change in the average weight loss, or any adverse effect of mice before and after the administration of $Eu^{III}(OH)_3$ for S-T and L-T toxicity studies even at highest dose (125 mg/Kg/day/mice). We have also collected and taken the weight of the specific organs (liver, kidney, lungs, spleen) after sacrificing the mice on day eight and day 60, and we have not observed any significant change of weight of different organs.

Blood tests done on day eight or 60 of the acute-toxicity experiments do not suggest any significant systemic toxicity at any of the dose levels (Table 1–4) except the slight elevation of liver enzymes, especially AST, for only the S-T toxicity study. In particular, even at the highest dose levels (dose125 $mgKg^{-1}day^{-1}$), inorganic nanorods do not cause anemia, neutropenia, lymphopenia, or thrombocytopenia suggestive of hematological toxicity (Table-1 and -3). The hematology and blood chemistry data of control mice are in the range with previously reported data (Hainfeld *et al.*, 2006). The normal range of creatinine and blood urea nitrogen (BUN) are between 0.2–0.4 mg dl^{-1} and 26–33 mg dl^{-1}, respectively (Hainfeld *et al.*, 2006). In our case, we have observed the normal value of creatinine and BUN are 0.1±0 mg dl^{-1} and 222±8, respectively. There is no difference in the value of BUN or creatinine in the blood of inorganic nanorod treated mice and control mice indicating no renal toxicity (Table-2 & -4) (Limpeanchob *et al.*, 2006). Liver enzymes are normally found within the cells of the liver. If the liver is injured or damaged, the liver enzymes spill into the blood, causing elevated liver enzyme levels. According to reported literature (Hainfeld *et al.*, 2006), the normal range of AST, ALT, ALP and AST/ALT in Balb/C mice are in the range of 38.8±9.9 to 123±52.5; 40.8±6.7 to 226±105; 100.4±28 to180±60; 1.8± 0.5 to 6.0± 2.5, respectively. There are slight elevations of liver enzymes, especially aspartate aminotransferase (AST) and alanine aminotransferase (ALT) in inorganic nanorod treated mice compared to untreated mice (Table-2). Although the AST level was increased (observed only for short term toxicity study; Table-2) in response to $Eu^{III}(OH)_3$ nanorods, bilirubin whole (0.1 mg/dL) is the most important factor for advanced liver toxicity and did not increase. Again, for the long-term (L-T) toxicity study we did not find any significant difference of ALT & AST values between control untreated mice and nanorod treated mice even at the high dose of 125 mg/Kg/day. The clinical significance of the increase in ALT & AST requires more investigation in future studies (Shah *et al.*, 2001). However, there is no significant change in the ratio of AST to ALT between controlled, untreated and nanorod treated mice for S-T and as well as L-T toxicity studies (Hainfeld *et al.*, 2006).

In human blood, albumin is the main protein (the primary component of total protein); and it is made by the liver. There is no change of albumin in nanorod treated mice compared to normal untreated mice indicating no liver disease which results in decreased albumin production. Elevated bilirubin levels can be indicative of liver disorders or blockage of bile ducts. However, we have not observed any elevation of bilirubin between control untreated mice and nanorod treated mice indicating no liver abnormalities. Other blood tests can also signal liver function problems by detecting abnormalities involving plasma proteins and blood clotting factors. No change of total protein plasma proteins (albumin and globulins) between control and nanorod treated mice indicating no abnormalities in liver even at highest dose of nanorod treatment. The inorganic phosphorous (P) in the form of phosphate has physiologic and pathologic importance in maintaining the neutrality of blood and tissue owing to a remarkable capacity for binding acid and base. In serum clinical chemistry data, total phosphorous, calcium, albumin, creatinine, glucose were not affected by the treatment of $Eu^{III}(OH)_3$ nanorods in mice compared to untreated mice. The combined blood hematology and serum clinical chemistry data (Table 1–4) do not show any sub clinical systemic toxicity detectable by our laboratory tests (Uckun *et al.*, 2002).

Short–term (S-T) and long-term (L-T)Histopathological Examination

Histological studies are considered to be a reliable method to detect structural changes due to toxicities(Reinders *et al.*, 2003). The histopathological findings of liver, kidney, spleen and lung for the S-T study are presented in Fig. 4.(a–p).

Lung histopathology

The sections from control animals are showing normal alveolar geometry and normal appearing alveolar septum (Fig. 4a). The same histopathological findings are seen after a dose of 1.25 $mg^{-1}kg^{-1}day^{-1}$ (Fig. 4b). With a dose of 12.5 $mg^{-1}kg^{-1}day,^{-1}$ mild thickening of the alveolar membrane and localized Para bronchiolar lipophagocytic changes were detected with both 12.5 $mg^{-1}kg^{-1}day^{-1}$ and 125 $mg^{-1}kg^{-1}day^{-1}$ doses indicating mild lung toxicity (Fig. 4c, d).

Liver histopathology

Sections from the control animals are showing normal hepatic architecture, hepatocytes, portal triad and central vein (Fig. 4e). The same histopathological findings are seen with 1.25 $mg^{-1}kg^{-1}day^{-1}$ (Fig. 4f). After a dose of 12.5 $mg^{-1}kg^{-1}day^{-1}$ mild hepatocytes cloudy swelling was observed (Fig. 4g). Sinusoidal congestion and mild lobular inflammation were also observed with a dosage of 125 $mg^{-1}kg^{-1}day,^{-1}$ indicating mild liver toxicity (Fig. 4h).

Kidney histopathology

Sections from the control animals are showing normal renal cortex with normal appearing glomerular tufts and tubules and normal renal papilla (Fig. 4i). After a dose of 1.25 $mg^{-1}kg^{-1}day,^{-1}$ still the sections are showing normal renal cortex with normal appearing glomerular tufts and tubules and normal renal papilla (Fig. 4j). Cloudy swelling in renal cortical tubular epithelium is seen at 12.5 $mg^{-1}kg^{-1}day^{-1}$ dose (Fig. 4k). Mild glomerular mesangial cell proliferation and arteriolar congestion are detected at 125 dose $mg^{-1}kg^{-1}day^{-1}$ dose (Fig. 4l).

Spleen histopathology

Sections from the control animals are showing normal splenic architecture with normal lymphoid follicles and sinuses (Fig. 4m). Normal histopathology findings are still seen after a dose of 1.25 $mg^{-1}kg^{-1}day^{-1}$ (Fig. 4n). No pathological changes are seen with a dose of 12.5 $mg^{-1}kg^{-1}day^{-1}$ (Fig. 4o). At a dose of 125 $mg^{-1}kg^{-1}day,^{-1}$ mild follicular hyperplasia is seen indicating mild toxicity of the spleen (Fig. 4p). The reported histopathological changes may

represent cellular compensatory changes to the injected nanorods and don't necessary indicate a toxic effect.

We have also examined the histologic specimens of vital tissues (liver, kidney, spleen and lung) collected from mice sacrificed on day 60 using H & E staining, and they showed normal histology of liver, kidney, spleen and lung (Fig. 5.a–l).

Bio-availabilities of europium

The europium element was detected in diverse organs such as liver, kidney, spleen and lungs (Fig. 6). The particles were distributed in all organs, and the distribution pattern was shown in Fig. 6. The concentration of europium element in different organs was analyzed by inductively coupled plasma mass spectrometry (ICPMS). The bio-distribution of europium element (per gram of tissue) in different organs of mice for short-term (ST; 7 days) and long-term (LT; 60 days) treatment with different doses (1.25 $mg^{-1}kg^{-1}day^{-1}$, 1.25 $mg^{-1}kg^{-1}day^{-1}$, 1.25 $mg^{-1}kg^{-1}day^{-1}$, and 125-L-T = 1.25 $mg^{-1}kg^{-1}day^{-1}$, long-term) after intra-peritoneal injection for seven days are shown in Fig. 6. The accumulated europium concentration in liver, kidney, spleen and lungs was ~440, ~788, ~4390 and ~75 μg/g of tissue, respectively, for the treatment of 125 $mg^{-1}kg^{-1}day^{-1}$ which is a very high dose. However, using the medium dose of $Eu^{III}(OH)_3$ nanorods (12.5 $mgKg^{-1}day^{-1}$) the concentration in liver, kidney, spleen and lungs was ~2, ~6, ~440 and ~6.2 μg/g of tissue, respectively. The distribution of europium in liver, kidney and lungs was almost negligible which is not damaging for liver, kidney, and lungs. The concentration of europium is higher in the spleen as compared to other organs at all doses of $Eu^{III}(OH)_3$ nanorods. These results support the reported literature (Nakamura *et al.*, 1997;Palasz and Czekaj, 2000). Nakamura *et al*. reported that lanthanide ions are cleared from blood within one day, but they remain much longer in the organs. Long-term toxicity testing of $Eu^{III}(OH)_3$ nanorods for more than 60 days also reveals the similar pattern of bio-distribution.

In our study, $Eu^{III}(OH)_3$ nanorods were administered to mice through the intraperitoneal (IP) route. Thus, the majority of the nanorods would be taken up by the liver via the first-pass effects and then redistributed from the liver to the other organs. Our results show that $Eu^{III}(OH)_3$ nanorods are rapidly and widely redistributed in the body except in the case of the lungs. We studied tissues that are enriched with the reticuloendothelial system (RES) such as the liver, spleen, and lungs and non-RES organs such as kidney. The highest concentrations of $Eu^{III}(OH)_3$ nanorods were observed in the liver and spleen. Among the RES organs, $Eu^{III}(OH)_3$ nanorods were distributed in small amounts only in the lungs, thereby suggesting that the localization of the $Eu^{III}(OH)_3$ nanorods in the liver, lungs, and spleen was not consistent with the RES system (Kim *et al.*, 2006). We have observed that high doses of $Eu^{III}(OH)_3$ nanorods (125 $mg^{-1}kg^{-1}day^{-1}$) have no lethal toxicity; even with long-term toxicity studies, there were no deaths of mice using high doses of inorganic nanorods for more than 60 days (100 % survival). It is reported that hydrodynamic size (Svedberg *et al.*, 2005) of nanoparticles (NPs) also affects NPs clearance from circulation (Moghimi, 1995a; Moghimi, 1995b; Moghimi and Hunter, 2001; Moghimi *et al.*, 2001; Choi *et al.*, 2007; Longmire *et al.*, 2008; Zamboni, 2008). For instance, it has been reported that small NPs (< 20 nm) are excreted renally, (Banerjee *et al.*, 2002; Choi *et al.*, 2007) while medium sized NPs (30–150 nm) have accumulated in the bone marrow, (Moghimi, 1995a) heart, kidney, and stomach; (Banerjee *et al.*, 2002) and large NPs (150–300 nm) have been found in the liver and spleen (Moghimi, 1995b). While these size ranges provide general clearance mechanisms, other physical parameters simultaneously affect NPs movement.

We have calculated the relative tissue distribution (i.e., how much of the dose was retrieved in the different tissues) and how much of the dose that is not accounted for. The persistence of europium in the body is an important parameter for determining a hazard. However, in this

article we have only focused on the effect of nanorods in a time dependent (8–60 days) and dose dependent manner (1.25–125 $mg^{-1}Kg^{-1}day^{-1}$) in animals. The clinical significance, biohazard, and long term persistence of europium in the body require more investigation in future studies.

The relative distribution pattern of the europium element in different vital organs is almost the same for the mice sacrificed on day eight as well as day 60. However, the amount of europium is less than in the latter case. We have calculated the amount of europium present in different tissues from the mice sacrificed on day eight (short-term study) and day 60 (long-term study), respectively. We have injected $Eu^{III}(OH)_3$ nanorods intraperitonially for seven days in each mouse (weight of each mice is ~25 g) at three doses such as 1.25 $mg^{-1}Kg^{-1}day^{-1}$(163.8 μg), 12.5 $mg^{-1}Kg^{-1}day^{-1}$(1638 μg), and 125 $mg^{-1}Kg^{-1}day^{-1}$(16380 μg), respectively. We have observed that total 3.2 wt. % (52.7 μg) and 8.2 wt. % (1338.2 μg) of europium is retained in the vital organs (liver, kidney, spleen and lung) from each mouse treated with nanorods at 12.5 $mg^{-1}Kg^{-1}day^{-1}$ and 125 $mg^{-1}Kg^{-1}day^{-1}$ for the short-term toxicity study. Similarly, we have found that only 3.3 wt. % (539.5 μg) of europium is retained in vital organs (liver, kidney, spleen and lung) of each mouse treated with nanorods at 125 $mg^{-1}Kg^{-1}day^{-1}$50 μg for 7 day injection). These observations indicate that with increasing time, retention of europium is decreased over time from eight days to 60 days. The rest of the europium (which we can't account for) is eliminated from the body maybe due to excretion (urine and feces) or accumulation in other parts of the body.

Our ultimate goal is to utilize the pro-angiogenic properties and non-toxic behavior of $Eu^{III}(OH)_3$ nanorods for future therapeutic treatment strategies of severe ischemic heart disease, peripheral ischemic disease, limb ischemic disease, etc. Our therapeutic dose of $Eu^{III}(OH)_3$ nanorods would be administered locally to the ischemic part of the disease at a microgram level which is at a far lower dose compared to the dose of our toxicity experiments (milligram level). As the therapeutic dose of $Eu^{III}(OH)_3$ nanorods is very low compared to the toxicity dose, we believe that these nanorods can be used safely for the treatment of several ischemic disease.

CONCLUSION

$Eu^{III}(OH)_3$ nanorods have been synthesized in our laboratory by microwave irradiation and characterized using several analytical tools. The as-synthesized materials are non-toxic to endothelial cells observed by apoptosis assay. Intraperitonial injection of $Eu^{III}(OH)_3$ nanorods at several doses in mice showed normal blood hematology and serum clinical chemistry except the slight elevation of liver enzymes. Histological examination of vital organs including liver, kidney, spleen, and lungs from each mouse, assayed on day eight or day 60 after injection of nanorods, showed none or only mild histological changes that indicates mild toxicity at highest dose of nanorods. Taken together, our results demonstrated that $Eu^{III}(OH)_3$ nanorods of 200–300-nm size caused no or mild toxicity under the experimental conditions of this study. The remarkable findings of pro-angiogenic properties and non-toxic behavior of $Eu^{III}(OH)_3$ nanorods suggests that these nanorods could be used for future therapeutic alternative treatment strategies for severe ischemic heart disease, peripheral ischemic disease, and limb ischemic disease.

Acknowledgments

The authors are also grateful to Prof. Rick A. Knurr of Department of Geology & Geophysics at University of Minnesota for ICPMS analysis and J. Charlesworth of the EM Core Facility at Mayo Clinic for the TEM analysis. We are also thankful to Mrs. Denise R Lecy and Colleen L. Allen for editorial assistance.

FUNDING SUPPORT

This work was partly supported by the National Institutes of Health (NIH) grant (HL70567 to D.M) and also partly supported by UOFM-MEDICA# 5P1, a grant from Minnesota Partnership for translational Nanotechnology in Cancer to P. M.

References

Alivisatos AP, Johnsson KP, Peng XG, Wilson TE, Loweth CJ, Bruchez MP, Schultz PG. Organization of 'nanocrystal molecules' using DNA. Nature 1996;382:609–611. [PubMed: 8757130]

Alivisatos P. The use of nanocrystals in biological detection. Nat Biotechnol 2004;22:47–52. [PubMed: 14704706]

Authors. Lanthanides in medicine special issue. Chem Soc Rev 2006;35:493–576.

Banerjee T, Mitra S, Singh AK, Sharma RK, Maitra A. Preparation, characterization and biodistribution of ultrafine chitosan nanoparticles. Int J Pharm 2002;243:93–105. [PubMed: 12176298]

Bruce DW, Hietbrink BE, DuBois KP. The acute mammalian toxicity of rare earth nitrates and oxides. Toxicol Appl Pharmacol 1963;5:750. [PubMed: 14082480]

Bruchez M, Moronne M, Gin P, Weiss S, Alivisatos AP. Semiconductor nanocrystals as fluorescent biological labels. Science 1998;281:2013–2016. [PubMed: 9748157]

Chavakis E, Dimmeler S. Regulation of endothelial cell survival and apoptosis during angiogenesis. Arterioscler Thromb Vasc Biol 2002;22:887–893. [PubMed: 12067894]

Chen JP, Patil S, Seal S, McGinnis JF. Rare earth nanoparticles prevent retinal degeneration induced by intracellular peroxides. Nature Nanotechnol 2006;1:142–150. [PubMed: 18654167]

Choi HS, Liu W, Misra P, Tanaka E, Zimmer JP, Ipe BI, Bawendi MG, Frangioni JV. Renal clearance of quantum dots. Nature Biotechnol 2007;25:1165–1170. [PubMed: 17891134]

Craighead, H. Applications: Biological, medical and health. Kluwer Academic Publishers; Boston: 2000.

Dardik R, Loscalzo J, Eskaraev R, Inbal A. Molecular mechanisms underlying the proangiogenic effect of factor XIII. Arterioscler Thromb Vasc Biol 2005;25:526–532. [PubMed: 15618543]

Derfus AM, Chan WCW, Bhatia SN. Probing the cytotoxicity of semiconductor quantum dots. Nano Lett 2004;4:11–18.

Ebrahimian TG, Heymes C, You D, Blanc-Brude O, Mees B, Waeckel L, Duriez M, Vilar J, Brandes RP, Levy BI, Shah AM, Silvestre JS. NADPH oxidase-derived overproduction of reactive oxygen species impairs postischemic neovascularization in mice with type 1 diabetes. American Journal of Pathology 2006;169:719–728. [PubMed: 16877369]

Fang YP, Xu AW, Song RQ, Zhang HX, You LP, Yu JC, Liu HQ. Systematic synthesis and characterization of single-crystal lanthanide orthophosphate nanowires. J Am Chem Soc 2003;125:16025–16034. [PubMed: 14677994]

Folkman J. Diagnostic and Therapeutic Applications of Angiogenesis Research. Comptes Rendus De L Academie Des Sciences Serie Iii-Sciences De La Vie-Life Sciences 1993;316:914–918.

Folkman J. Angiogenesis in Cancer, Vascular, Rheumatoid and Other Disease. Nat Med 1995;1:27–31. [PubMed: 7584949]

Folkman J. Tumor ngiogenesis: role in regulation of tumor growth. Symp Soc Dev Biol 1974;30:43–52. [PubMed: 4600889]

Folkman J, Shing Y. Angiogenesis. J Biol Chem 1992;267:10931–10934. [PubMed: 1375931]

Gao XH, Cui YY, Levenson RM, Chung LWK, Nie SM. In vivo cancer targeting and imaging with semiconductor quantum dots. Nat Biotechnol 2004;22:969–976. [PubMed: 15258594]

Gao XH, Yang LL, Petros JA, Marshal FF, Simons JW, Nie SM. In vivo molecular and cellular imaging with quantum dots. Curr Opin Biotechnol 2005;16:63–72. [PubMed: 15722017]

Hainfeld JF, Slatkin DN, Focella TM, Smilowitz HM. Gold nanoparticles: a new X-ray contrast agent. Br J Radiol 2006;79:248–253. [PubMed: 16498039]

Haley TJ, Komesu N, Colvin G, Koste L, Upham HC. Pharmacology and toxicology of europium chloride. J Pharma Sci 1965;54:643–645.

Hirano S, Suzuki KT. Exposure, Metabolism, and Toxicity of Rare Earths and Related Compounds. Environ Health Perspect Suppl 1996;104:85–95.

Huang MH, Mao S, Feick H, Yan HQ, Wu YY, Kind H, Weber E, Russo R, Yang PD. Room-temperature ultraviolet nanowire nanolasers. Science 2001;292:1897–1899. [PubMed: 11397941]

Huston SL, Lengerich EJ, Conlisk E, Passaro K. Trends in ischemic heart disease death rates for blacks and whites United States, 1981–1995 (Reprinted from MMWR, vol 47, pg 945–949, 1998). Jama-Journal of the American Medical Association (JAMA) 1999;281:28–29.

Isner JM, Losordo DW. Therapeutic angiogenesis for heart failure. Nat Med 1999;5:491–492. [PubMed: 10229223]

Jain KK. Nanotechnology in clinical laboratory diagnostics. Clin Chim Acta 2005a;358:37–54. [PubMed: 15890325]

Jain KK. Nanotechnology-based Drug Delivery for Cancer. Technol Cancer Res Treat 2005b;4:407–416. [PubMed: 16029059]

Jaiswal JK, Mattoussi H, Mauro JM, Simon SM. Long-term multiple color imaging of live cells using quantum dot bioconjugates. Nat Biotechnol 2003;21:47–51. [PubMed: 12459736]

Jones DW, Chambless LE, Folsom AR, Heiss G, Hutchinson RG, Sharrett AR, Szklo M, Taylor HA. Risk factors for coronary heart disease in African Americans - The Atherosclerosis Risk in Communities Study, 1987–1997. Arch Int Med 2002;162:2565–2571. [PubMed: 12456228]

Kim JS, Yoon dagger TJ, Yu KN, Kim BG, Park SJ, Kim HW, Lee KH, Park SB, Lee JK, Cho MH. Toxicity and Tissue Distribution of Magnetic Nanoparticles in Mice. Toxicol Sci 2006;89:338–347.10.1093/toxsci/kfj027 [PubMed: 16237191]

Limpeanchob N, Tiyaboonchai W, Lamlertthon S, Viyoch J, Jaipan S. Efficacy and Toxicity of Amphotericin B-Chitosan Nanoparticles in Mice with Induced Systemic Candidiasis. Naresuan University Journal 2006;14:27–34.

Longmire M, Choyke PL, Kobayashi H. Clearance properties of nano-sized particles and molecules as imaging agents: considerations and caveats. Nanomedicine 2008;3:703–717. [PubMed: 18817471]

Matsumurainoue T, Tanabe M, Minami T, Ohashi T. A Remarkably Rapid Synthesis of Ruthenium(Ii) Polypyridine Complexes by Microwave Irradiation. Chem Lett 1994:2443–2446.

Mazloumi M, Shahcheraghi N, Kajbafvala A, Zanganeh S, Lak A, Mohajerani MS, Sadrnezhaad SK. 3D bundles of self-assembled lanthanum hydroxide nanorods via a rapid microwave-assisted route. J Alloys Comp 2009;473:283–287.

McDowell EM, Trump BF. Histologic fixatives suitable for. diagnostic light and electron microscopy. Arch Path Lab Med 1976;10:405–414. [PubMed: 60092]

Medintz IL, Uyeda HT, Goldman ER, Mattoussi H. Quantum dot bioconjugates for imaging, labelling and sensing. Nat Mater 2005;4:435–446. [PubMed: 15928695]

Michalet X, Pinaud FF, Bentolila LA, Tsay JM, Doose S, Li JJ, Sundaresan G, Wu AM, Gambhir SS, Weiss S. Quantum dots for live cells, in vivo imaging, and diagnostics. Science 2005;307:538–544. [PubMed: 15681376]

Misra SN, Gagnani MA, Devi I, Shukla RS. Biological and clinical aspects of lanthanide coordination compounds. Bioinorg Chem Appl 2004;2:155–192. [PubMed: 18365075]

Moghimi SM. Exploiting Bone-Marrow Microvascular Structure for Drug-Delivery and Future Therapies. Adv Drug Deliv Rev 1995a;17:61–73.

Moghimi SM. Mechanisms of Splenic Clearance of Blood-Cells and Particles - Towards Development of New Splenotropic Agents. Adv Drug Deliv Rev 1995b;17:103–115.

Moghimi SM, Hunter AC. Capture of stealth nanoparticles by the body's defences. Crit Rev Ther Drug Carrier Syst 2001;18:527–550. [PubMed: 11789674]

Moghimi SM, Hunter AC, Murray JC. Long-circulating and target-specific nanoparticles: Theory to practice. Pharmacol Rev 2001;53:283–318. [PubMed: 11356986]

Nakamura Y, Tsumura Y, Shibata T, Ito Y. Differences in behavior among the chlorides of seven rare earth elements administered intravenously to rats. Toxicol 1997:37.

Ogawa Y, Suzuki S, Naito K, Saito M, Kamata E, Hirose A, Ono A, Kaneko T, Chiba M, Inaba Yea. Toxicity study of europium chloride in rats. J-Environ-Pathol-Toxicol-Oncol 1995;14:1–19. [PubMed: 7473067]

Palasz A, Czekaj P. Toxicological and cytophysiological aspects of lanthanides action. Acta Biochimica Polonica 2000;47:1107–1114. [PubMed: 11996100]

Parak WJ, Gerion D, Pellegrino T, Zanchet D, Micheel C, Williams SC, Boudreau R, Le Gros MA, Larabell CA, Alivisatos AP. Biological applications of colloidal nanocrystals. Nanotechnology 2003;14:R15–R27.

Patra CR, Alexandra G, Patra S, Jacob DS, Gedanken A, Landau A, Gofer Y. Microwave approach for the synthesis of rhabdophane-type lanthanide orthophosphate (Ln = La, Ce, Nd, Sm, Eu, Gd and Tb) nanorods under solvothermal conditions. New J Chem 2005;29:733–739.

Patra CR, Bhattacharya R, Mukhopadhyay D, Mukherjee P. Application of gold nanoparticles for targeted therapy in cancer. J Biomed Nanotechnol 2008a;4:99–132.

Patra CR, Bhattacharya R, Patra S, Basu S, Mukherjee P, Mukhopadhyay D. Inorganic phosphate nanorods are a novel fluorescent label in cell biology. J Nanobiotechnology 2006:4. [PubMed: 16603066]

Patra CR, Bhattacharya R, Patra S, Basu S, Mukherjee P, Mukhopadhyay D. Lanthanide phosphate nanorods as inorganic fluorescent labels in cell biology research. Clin Chem 2007;53:2029–2031. [PubMed: 18035595]

Patra CR, Bhattacharya R, Patra S, Vlahakis NE, Gabashvili A, Koltypin Y, Gedanken A, Mukherjee P, Mukhopadhyay D. Pro-angiogenic properties of europium(III) hydroxide nanorods. Adv Mater 2008b;20:753–756.

Patra CR, Bhattacharya R, Wang E, Katarya A, Lau JS, Dutta S, Muders M, Wang S, Buhrow SA, Safgren SL, Yaszemski MJ, Reid JM, Ames MM, Mukherjee P, Mukhopadhyay D. Targeted delivery of gemcitabine to pancreatic adenocarcinoma using cetuximab as a targeting agent. Cancer Res 2008c; 68:1970–1978. [PubMed: 18339879]

Patra CR, Cao S, Safgren S, Bhattacharya R, Ames M, Shah V, Reid JM, Mukherjee P. Intracellular Fate of a Targeted Delivery System. J Biomed Nanotechnol 2008d;4:508–514.

Patra, CR.; Mukherjee, P.; Mukhopadhyay, D. *Application of Lanthanide (Ln = Eu & Tb) Nanoparticles in Biology and Medicine*. Nova Science Publishers; NY: 2009.

Patra CR, Verma R, Kumar S, Greipp PR, Mukhopadhyay D, Mukherjee P. Fabrication of Gold Nanoparticle for Potential Application in Multiple Myeloma. J Biomed Nanotechnol 2008e;4:499–507.

Prescher JA, Bertozzi CR. Chemistry in living systems. Nat Chem Biol 2005;1:13–21. [PubMed: 16407987]

Reinders MEJ, Sho M, Izawa A, Wang P, Mukhopadhyay D, Koss KE, Geehan CS, Luster AD, Sayegh MH, Briscoe DM. Proinflammatory functions of vascular endothelial growth factor in alloimmunity. J Clin Invest 2003;112:1655–1665. [PubMed: 14660742]

Risau W. Mechanisms of angiogenesis. Nature 1997;386:671–674. [PubMed: 9109485]

Roco MC. Nanotechnology: Convergence with modern biology and medicine. Curr Opin Biotechnol 2003;14:337–346. [PubMed: 12849790]

Shah V, Cao S, Hendrickson H, Yao J, Katusic ZS. Regulation of hepatic eNOS by caveolin and calmodulin after bile duct ligation in rats. Am J Physiol-Gastrointest Liver Physiol 2001;280:G1209–G1216. [PubMed: 11352814]

Shimada H, Nagano M, Funakoshi T, Kojima S. Pulmonary toxicity of systemic terbium chloride in mice. J Toxicol Environ Health 1996;48:81–92. [PubMed: 8637060]

Sigel, A.; Sigel, H. Metal Complexes in Tumor Diagnosis and as Anticancer Agents. Marcel Dekker; New York: 2004.

Spurr AR. A low viscosity epoxy resin embedding medium for electron microscopy. J Ultrastruct Res 1969;26:31–36. [PubMed: 4887011]

Svedberg EB, Ahner J, Shukla N, Ehrman SH, Schilling K. FePt nanoparticle hydrodynamic size and densities from the polyol process as determined by analytical ultracentrifugation. Nanotechnology 2005;16:953–956.

Thompson KH, Orvig C. Editorial: Lanthanide compounds for therapeutic and diagnostic applications. Chem Soc Rev 2006;35:499–499. [PubMed: 16729143]

Thrall JH. Nanotechnology and medicine. Radiology 2004;230:315–318. [PubMed: 14752175]

Uckun FM, Qazi S, Pendergrass S, Lisowski E, Waurzyniak B, Chen CL, Venkatachalam TK. In Vivo Toxicity, Pharmacokinetics, and Anti-Human Immunodeficiency Virus Activity of Stavudine-5′-(p-

Bromophenyl Methoxyalaninyl Phosphate) (Stampidine) in Mice. Antimicrob Agents and Chemother 2002;6:3428–3436. [PubMed: 12384347]

Wang X, Li YD. Synthesis and characterization of lanthanide hydroxide single-crystal nanowires. Angew Chem-Int Ed 2002;41:4790–4793.

Wu S, Ko YS, Teng MS, Ko YL, Hsu LA, Hsueh C, Chou YY, Liew CC, Lee YS. Adriamycin-induced cardiomyocyte and endothelial cell apoptosis: in vitro and in vivo studies. J Mol Cell Cardiol 2002;34:1595–1607. [PubMed: 12505058]

Xu AW, Fang YP, You LP, Liu HQ. A simple method to synthesize Dy(OH)(3) and DY2O3 nanotubes. J Am Chem Soc 2003;125:1494–1495. [PubMed: 12568606]

Yancopoulos GD, Davis S, Gale NW, Rudge JS, Wiegand SJ, Holash J. Vascular-specific growth factors and blood vessel formation. Nature 2000;407:242–248. [PubMed: 11001067]

Yu JH, Parker D, Pal R, Poole RA, Cann MJ. A europium complex that selectively stains nucleoli of cells. J Am Chem Soc 2006;128:2294–2299. [PubMed: 16478184]

Zamboni WC. Concept and clinical evaluation of carrier-mediated anticancer agents. Oncologist 2008;13:248–260. [PubMed: 18378535]

Zhang J, Campbell RE, Ting AY, Tsien RY. Creating new fluorescent probes for cell biology. Nat Rev Mol Cell Biol 2002;3:906–918. [PubMed: 12461557]

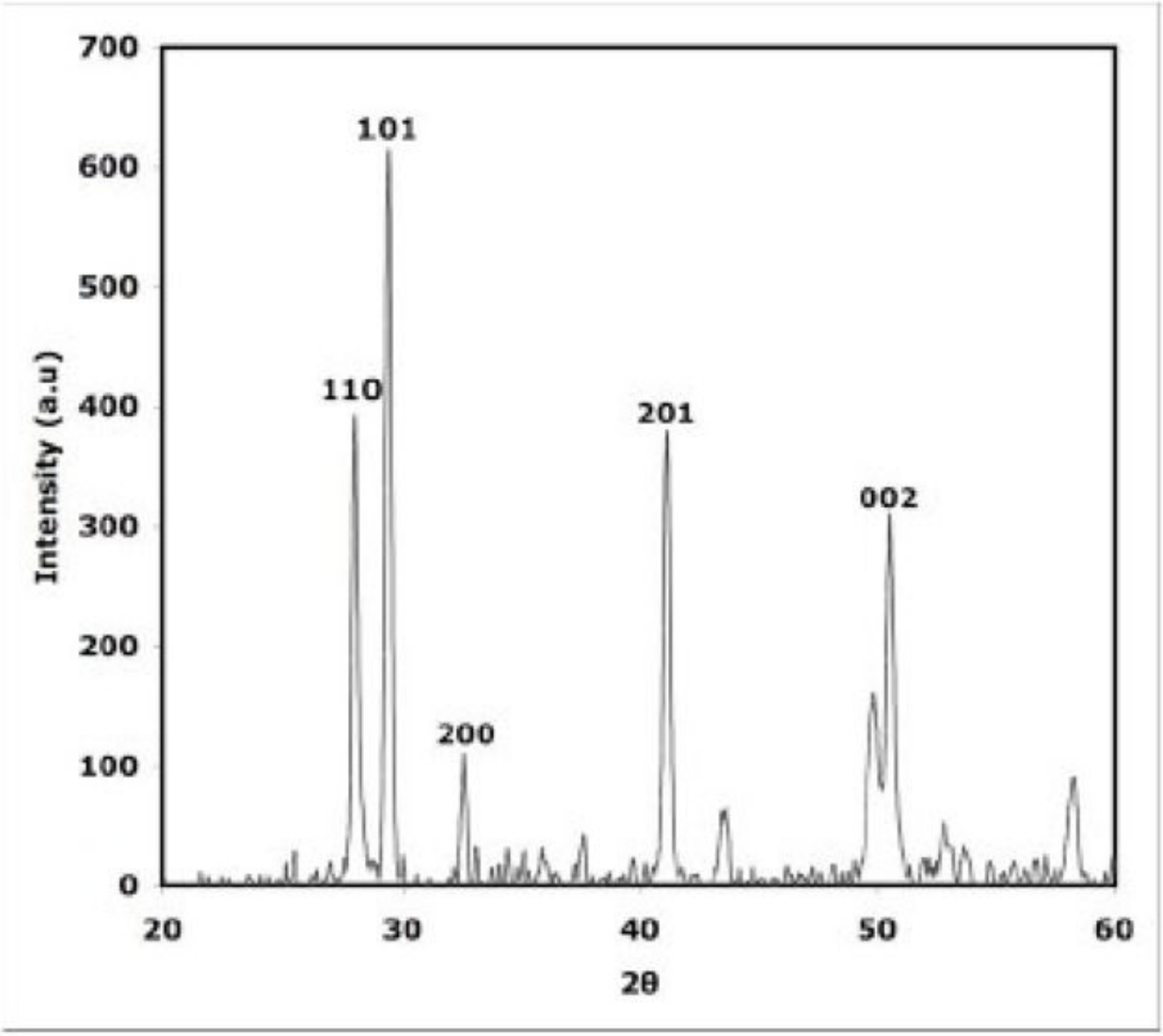

Fig. 1.

XRD patterns of as-synthesized nanorods, obtained after 60 mins of MW heating indicating that as-synthesized material is crystalline Eu $^{III}(OH)_3$ nanorods.

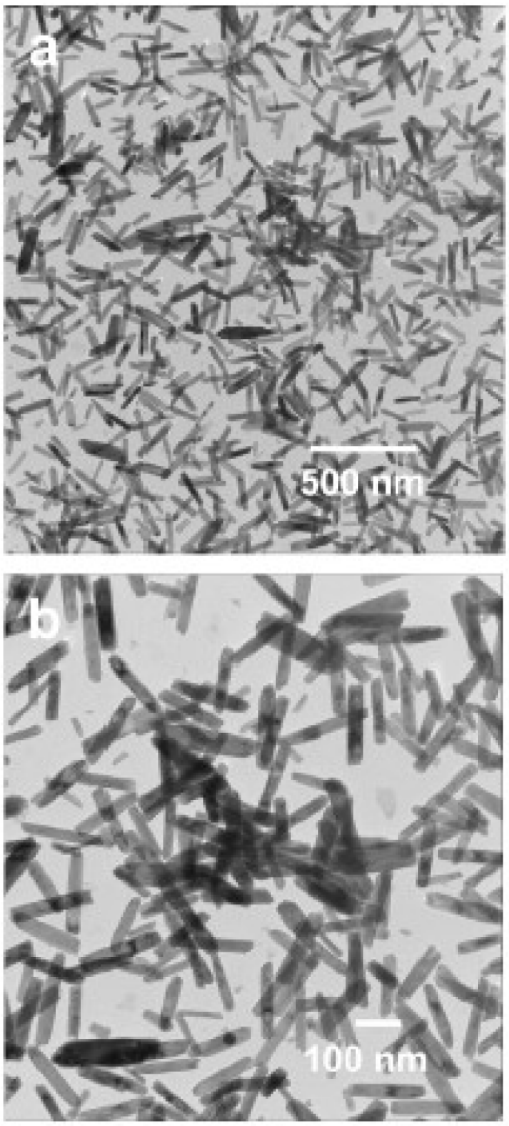

Fig. 2.
TEM image of the as-synthesized Eu $^{III}(OH)_3$ nanorods obtained after 60 min of microwave heating. The pictures show that as-synthesized materials entirely consist of nanorods with a diameter 35–50 nm and length in 200–300 nm.

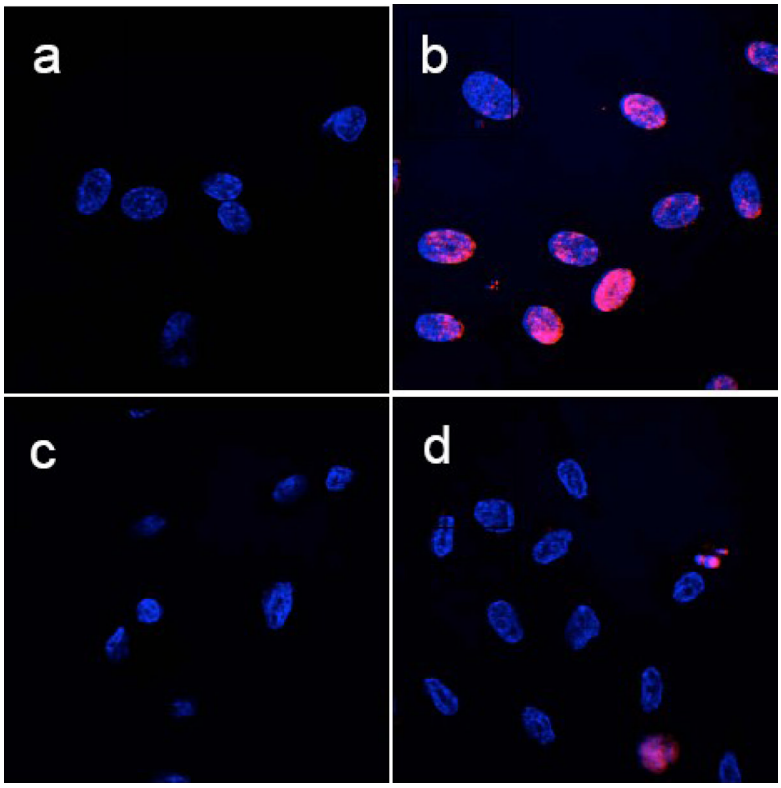

Fig. 3.

TUNEL assay experiments for apoptosis of HUVECs. (a) HUVECs treated with only Tris-EDTA buffer, (b) HUVECs treated with camptothecin for 4h at 37°C as a positive inducer. (c) HUVECs treated with $Eu^{III}(OH)_3$ nanorods (50 μg/mL) and (d) HUVECs treated with $Eu^{III}(OH)_3$ nanorods (50 μg/mL). TMR red-stained nuclei and DAPI stained nuclei of HUVECs appear in red (due to presence of apoptotic cells) and blue color, respectively. All pictures (a–d) are merged pictures of TMR red-stained nuclei and DAPI-stained nuclei of HUVEC.

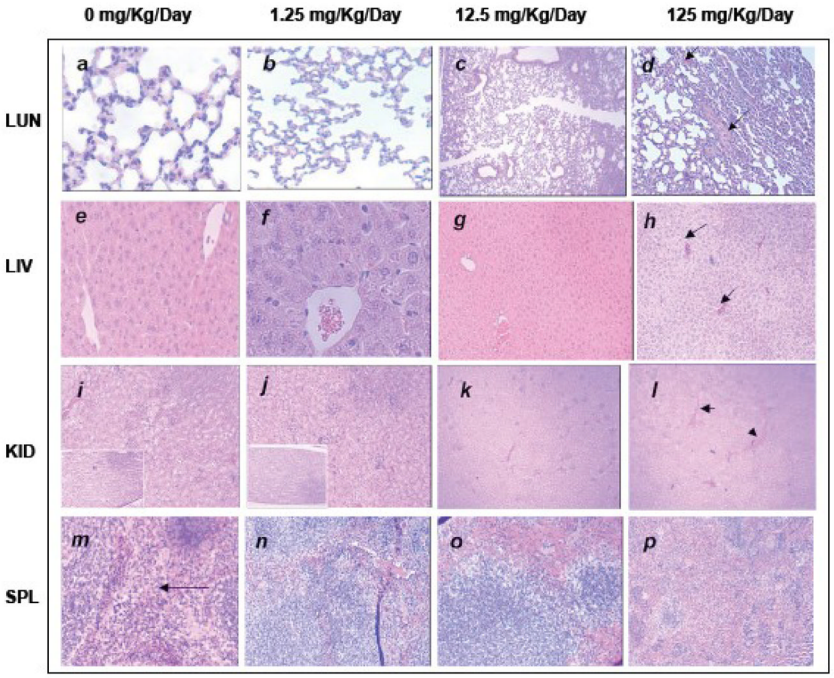

Fig. 4.

Histologic specimens of mice tissues (lung, liver, kidney and spleen) collected from mice sacrificed on day eight, stained with hematoxylin and eosin (H & E). Histological examination of liver, kidney, spleen, and lungs from nanorod treated mice, showed none or only mild histological changes that indicates mild toxicity at higher doses of nanorods. 100% survival of mice was observed even at highest dose of $Eu^{III}(OH)_3$ nanorods (125 mg $Kg^{-1}day^{-1}$) over more than 60 days of study. a. Control animal lung section showing normal alveolar geometry and normal appearing alveolar septum. b. Normal alveolar geometry and normal appearing alveolar septum with a dose of 1.25 $mg^{-1}kg^{-1}day^{-1}$. c. Mild thickening of the alveolar membrane is shown (arrow) with a dose of 12.5 $mg^{-1}kg^{-1}day^{-1}$. d. Parabronchiolar lipophagocytic change (arrow) is detected with a 125 $mg^{-1}kg^{-1}day^{-1}$ dose. e. Control animal liver section showing normal hepatic architecture, hepatocytes, portal triad, and central vein. f. Normal hepatic architecture, hepatocytes, portal triad and central vein are seen with 1.25 $mg^{-1}kg^{-1}day^{-1}$. g. Mild hepatocytes cloudy swelling (arrow) is observed after a dose of 12.5 $mg^{-1}kg^{-1}day^{-1}$. h. Hepatic sinusoidal congestion (arrow) and mild lobular inflammation were also observed (left bottom) with 125 $mg^{-1}kg^{-1}day^{-1}$. i. Kidney sections from the control animals are showing normal renal cortex with normal appearing glomerular tufts and tubules and normal renal papilla (left bottom). j. Kidney sections are showing normal renal cortex with normal appearing glomerular tufts and tubules and normal renal papilla (left bottom) after a dose of 1.25 $mg^{-1}kg^{-1}day^{-1}$. k. Cloudy swelling in renal cortical tubular epithelium (arrow) is seen at 12.5 $mg^{-1}kg^{-1}day^{-1}$ dose. l. Mild glomerular mesangial cells proliferation (thin arrow) and arteriolar congestion (thick arrow) are detected at 125 dose $mg^{-1}kg^{-1}day^{-1}$ dose. m. Splenic sections from the control animals are showing normal splenic architecture with normal lymphoid follicles and sinuses (arrow). n. Normal histopathologic findings are still seen after a dose of 1.25 $mg^{-1}kg^{-1}day^{-1}$. o. No pathological changes are seen with a dose of 12.5 $mg^{-1}kg^{-1}day^{-1}$. p. At a dose of 125 $mg^{-1}kg^{-1}day, ^{-1}$ mild follicular hyperplasia is seen. The histological pictures were taken at following magnifications: a- > x40, b- > x100, c- > x10, d-> x40, e-> x40, f- > x100, g-> x10, h- > x10, i- > x40, j- > x 40, k- > x10, l-> x10, m- > x100, n-> x 40, o- > x40, p- > x10.

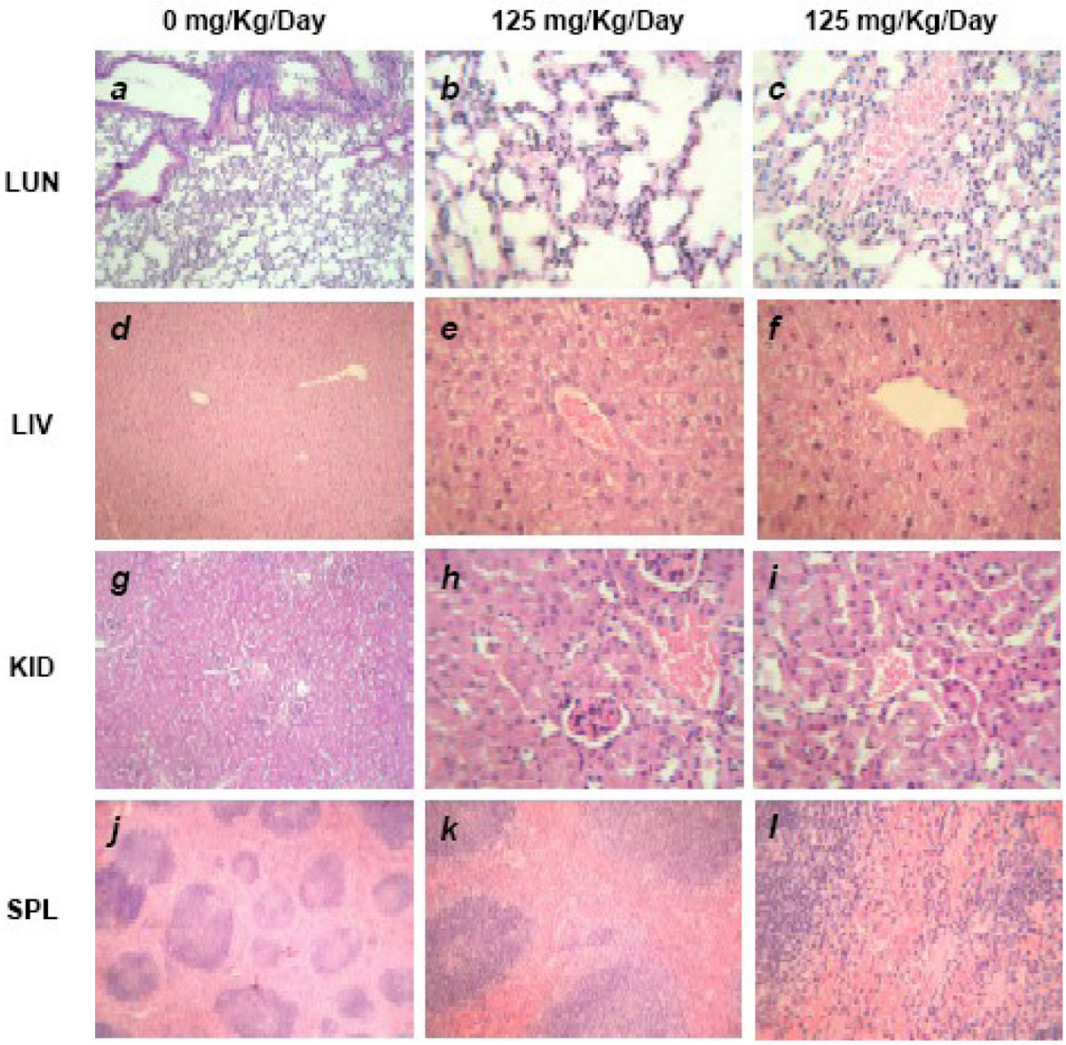

Fig. 5.

Histologic specimens of mice tissues (lung, liver, kidney and spleen) collected from mice sacrificed on day 60 stained with hematoxylin and eosin (H & E) showed normal histology. 100% long term survival of mice was also observed even at highest does of $Eu^{III}(OH)_3$ nanorods (125 mg $Kg^{-1}day^{-1}$). a. Control animal lung section showing normal alveolar geometry and normal appearing alveolar septum. b. Normal alveolar geometry and normal appearing alveolar septum with dose of 125 $mg^{-1}kg^{-1}day^{-1}$. c. Normal lung parenchymal blood vessels with dose of 125 $mg^{-1}kg^{-1}day^{-1}$. d. Control animal liver section showing normal hepatic architecture e. Normal portal tract, sinusoids and hepatocytes with dose of 125 $mg^{-1}kg^{-1}day^{-1}$. f. Normal central vein with dose of 125 $mg^{-1}kg^{-1}day^{-1}$. g.. Kidney sections from the control animals are showing normal renal cortex with normal appearing glomerular tufts and tubules. h. Normal appearing glomerular tufts with dose of 125 $mg^{-1}kg^{-1}day^{-1.}$ i. Normal appearing renal tubules and blood vessels. j. Splenic sections from the control animals are showing normal splenic lymphoid follicles. k. Normal splenic lymphoid follicles after a dose of 1.25 $mg^{-1}kg^{-1}day^{-1}$ l. Normal splenic sinuses are still seen after a dose of 1.25 $mg^{-1}kg^{-1}day^{-1}$. The histological pictures were taken at following magnifications: a- > x10, b- and c-> x100, d-> x40, e- and f- > x100, g-> x40, h- and i-> x100, j- > x10, k-> x 40, i- > x100.

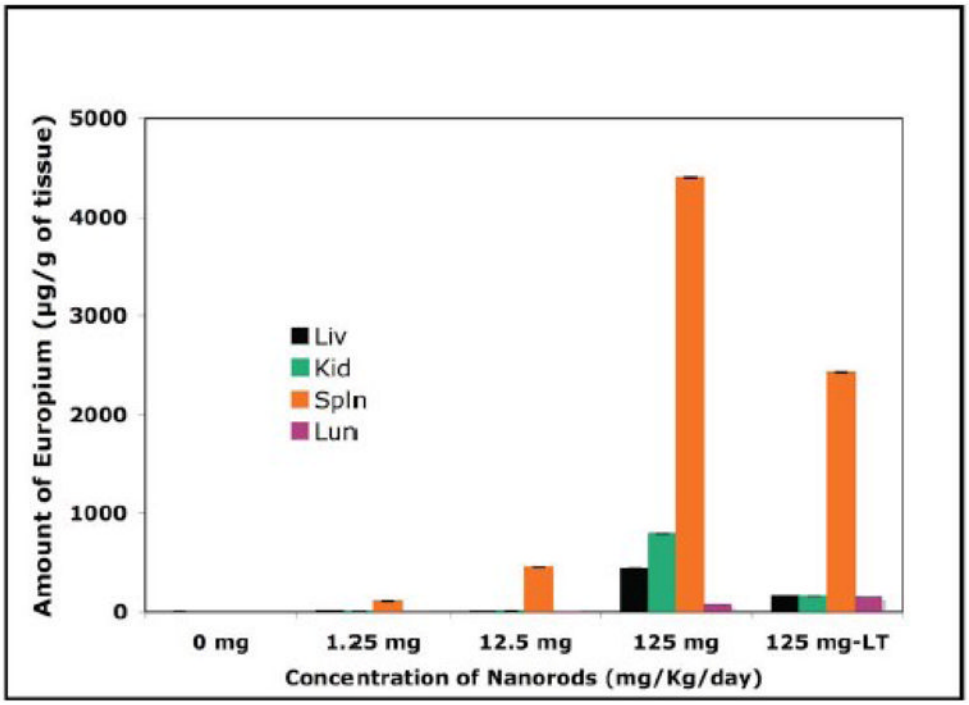

Fig. 6.

ICPMS data shows the bio-distribution of europium element (per gram of tissue) in different organs (LUN: lung; LIV: liver; KID: kidney; SPL: spleen) of mice, sacrificed on day eight (Short-term toxicity study) and 60 (Long-term toxicity study) after intra-peritonial injection for seven days with 0 (−ve control, 0.1ml of TE buffer), 1.25 mg $Kg^{-1}day^{-1}$ (= 1.25), 12.5 mg $Kg^{-1}day^{-1}$ (= 12.5), 125 mg $Kg^{-1}day^{-1}$ (=125) and 125 mg $Kg^{-1}day^{-1}$ (= 125-L-T; long-term) of $Eu^{III}(OH)_3$ nanorods suspended in TE buffer.

Table 1

Short term (S-T) toxicity Study

Blood hematology of mice after intra-peritonial injection with 0 (−ve control, 0.1ml of TE buffer), 1.25 mg $Kg^{-1}day^{-1}$ (0.1 ml), 12.5 mg $Kg^{-1}day^{-1}$ (0.1ml) and 125 mg $Kg^{-1}day^{-1}$ (0.1ml) of europium hydroxide nanorods suspended in TE buffer in the blood, sampled at 8 days. 10 animals were used per measurements, and all values were within normal rage.

	Control (TE buffer)	**1.25 mg $Kg^{-1}day^{-1}$**	**12.5 mg $Kg^{-1}day^{-1}$**	**125 mg $Kg^{-1}day^{-1}$**
CBC without differential hemoglobin (g/dL)	12.1 (± 0.6)	11.9 (± 0.4)	11.9 (± 0.7)	12.4 (± 0.5)
Hematocrit (%)	34.4 (± 1.1)	34.1 (± 1.0)	34.5 (± 1.5)	35.3 (± 1.5)
Erythrocytes [x10(12)/L]	7.5 (± 0.3)	7.4 (± 0.2)	7.6 (± 0.4)	7.9 (± 0.3)
MCV (fL)	45.8 (± 0.4)	45.9 (± 0.4)	45.4 (± 0.4)	44.9 (± 0.4)
RBC Distrib Width (%)	37.5 (± 1.7)	37.0 (± 2.3)	36.4 (± 0.2)	39.7 (± 0.9)
Leukocytes [x10(9)/L]	1.5 (± 0.3)	0.8 (± 0.1)	1.7 (± 0.6)	1.7 (± 0.2)
Platelet count [x10(9)/L]	844.7 (± 269)	804.5 (± 73.7)	807(± 301)	831 (± 175.6)

CBC: Complete blood, count; MCV: mean cell volume; RBC: Red blood cells. Numerical values (±) in the parenthesis are considered as ‘Standard Deviation (SD)’. P values were calculated using ‘Student-Newman-Keuls Multiple Comparisons Test ‘ (ANOVA) by comparing between different groups (control group vs treatment groups) and we found that these values are considered not significant ($P > 0.05$).

Toxicol Appl Pharmacol. Author manuscript; available in PMC 2010 October 1.

Table 2

Short term (S-T) toxicity Study

Serum clinical chemistry of mice after intra-peritonial injection with 0 (−ve control, 0.1ml of TE buffer), 1.25 mg $Kg^{-1}day^{-1}$ (0.1 ml), 12.5 mg $Kg^{-1}day^{-1}$ (0.1ml) and 125 mg $Kg^{-1}day^{-1}$ (0.1ml) of europium hydroxide nanorods suspended in TE buffer in the blood, sampled at 8 days. 10 animals were used per measurements, and all values were within normal rage.

	Control	**1.25 mg $Kg^{-1}day^{-1}$**	**12.5 mg $Kg^{-1}day^{-1}$**	**125 mg$Kg^{-1}day^{-1}$**
ALP (u/L)	123.0 (± 8.6)	122.4 (± 7.3)	132.8 (± 10.1)	95.2 (± 16.7)
AST (u/L)	158.0 (± 77.7)	250.8 (±60.9)	236.6 (± 71.5)	225.8 (± 86)
ALT (u/L)	49.4 (± 15.5)	105 (± 60.5)	63.8 (± 37.0)	74.0 (± 50.1)
AST/ALT (ratio)	3.2	2.4	3.7	3.1
Phosphorous (mg/dL)	11.0 (± 0.6)	11.7 (± 0.5)	11.2 (± 2.1)	11.2 (± 3)
Calcium (mg/dL)	9.4 (± 0.1)	9.4 (± 0.2)	9.3 (± 0.1)	9.6 (± 0.2)
Albumin (g/dL)	3.2 (± 0.1)	3.3 (± 0.1)	3.0 (± 0.2)	2.9 (± 0.1)
Creatinine, P/S (mg/dL)	0.1 (± 0.0)	0.1 (± 0.0)	0.1 (± 0.0)	0.1 (± 0.0)
Glucose (mg/dL)	209.2 (± 43.9)	222.4 (± 42.9)	216.6 (± 63)	191.8 (± 55.9)
Protein-total (g/dL)	4.6 (± 0.2)	4.6 (± 0.1)	4.4 (± 0.2)	4.4 (± 0.1)
Bilirubin total, S (mg/dL)	0.1 (± 0.0)	0.1 (± 0.0)	0.1 (± 0.0)	0.1 (± 0.0)
BUN) (mg/dL)	22.8 (± 2)	23.8 (± 2)	22.0 (± 2)	20.4 (± 2.6)

ALP: Alkaline phosphates, AST: Aspartate Aminotransferase, ALT: Alanine Aminotransferase, BUN: Blood Urea nitrogen. Numerical values (±) in the parenthesis are considered as ‘Standard Deviation (SD)’. P values were calculated using ‘Student-Newman-Keuls Multiple Comparisons Test ‘ (ANOVA) by comparing between different groups (control group vs treatment groups) and we found that these values are considered not significant ($P > 0.05$).

Table 3

Long term (S-T) toxicity Study

Blood hematology of mice after intra-peritonial injection with 0 (−ve control, 0.1ml of TE buffer), 1.25 mg $Kg^{-1}day^{-1}$ (0.1 ml), 12.5 mg $Kg^{-1}day^{-1}$ (0.1ml) and 125 mg $Kg^{-1}day^{-1}$ (0.1ml) of europium hydroxide nanorods suspended in TE buffer in the blood, sampled at 60 days. 10 animals were used per measurements, and all values were within normal rage.

	Control (TE buffer)	**125 mg $Kg^{-1}day^{-1}$**
CBC without differential hemoglobin (g/dL)	10.7 (± 1.3)	11.1 (± 0.6)
Hematocrit (%)	29.5 (± 3.5)	31.1 (± 1.3
Erythrocytes [x10(12)/L]	6.5 (± 0.8)	7.1 (± 0.3)
MCV (fL)	45.2 (± 0.8)	44.0 (± 0.4)
RBC Distrib Width (%)	33.1 (± 7.1)	37.0 (± 2.5)
Leukocytes [x10(9)/L]	2.0 (± 0.6)	2.2 (± 0.8)
Platelet count [x10(9)/L]	943.0 (± 52.9)	1037.2 (± 46.1)

CBC: Complete blood, count; MCV: mean cell volume; RBC: Red blood cells. Numerical values (±) in the parenthesis are considered as ‘Standard Deviation (SD)’. P values were calculated using ‘Student-Newman-Keuls Multiple Comparisons Test ‘ (ANOVA) by comparing between different groups (control group vs treatment groups) and we found that these values are considered not significant ($P > 0.05$).

Toxicol Appl Pharmacol. Author manuscript; available in PMC 2010 October 1.

Table 4

Short term (S-T) toxicity Study

Serum clinical chemistry of mice after intra-peritonial injection with 0 (−ve control, 0.1ml of TE buffer), 1.25 mg $Kg^{-1}day^{-1}$ (0.1 ml), 12.5 mg $Kg^{-1}day^{-1}$ (0.1ml) and 125 mg $Kg^{-1}day^{-1}$ (0.1ml) of europium hydroxide nanorods suspended in TE buffer in the blood, sampled at 60 days. 10 animals were used per measurements, and all values were within normal rage.

	Control (TE buffer)	**125 mg $Kg^{-1}day^{-1}$**
ALP (u/L)	53.4 (± 3.5)	65.8 (± 5.1)
AST (u/L)	131.6 (± 44.17)	133.2 (± 37.2)
ALT (u/L)	54.6 (± 11.2)	57.0 (± 12.1)
AST/ALT (ratio)	2.4	2.3
Phosphorous (mg/dL)	7.0 (± 0.6)	7.2 (± 1.1)
Calcium (mg/dL)	8.8 (± 0.1)	8.9 (± 0.1)
Albumin (g/dL)	3.1 (± 0.1)	3.0 (± 0.1)
Creatinine, P/S (mg/dL)	0.1 (± 0.0)	0.1 (± 0.0)
Glucose (mg/dL)	349.4 (± 46.3)	321.0 (± 39.88)
Protein-total (g/dL)	4.2 (± 0.1)	4.4 (± 0.2)
Bilirubin total, S (mg/dL)	0.1 (± 0.0)	0.1 (± 0.0)
BUN) (mg/dL)	23.0 (± 0.6)	20.0 (± 1.7)

ALP: Alkaline phosphates, AST: Aspartate Aminotransferase, ALT: Alanine Aminotransferase, BUN: Blood Urea nitrogen. Numerical values (±) in the parenthesis are considered as ‘Standard Deviation (SD)’. P values were calculated using ‘Student-Newman-Keuls Multiple Comparisons Test ‘ (ANOVA) by comparing between different groups (control group vs treatment groups) and we found that these values are considered not significant ($P > 0.05$).